

DISCRETE ELEMENT MODELING: A PROMISING WAY TO ACCOUNT EFFECTS OF DAMAGES GENERATED BY LOCAL THERMAL EXPANSION MISMATCHES ON MACROSCOPIC BEHAVIOR OF REFRACTORY MATERIALS

Truong Thi Nguyen¹, Damien André¹, Nicolas Tessier-Doyen¹ and Marc Huger¹

¹Science of Ceramic Processing and Surface Treatments (SPCTS), Limoges, France
truong_thi.nguyen@unilim.fr

ABSTRACT

For thermo-mechanical modeling of industrial vessels with the Finite Element Method (FEM), refractories should be seen, at macroscopic scale, as a homogeneous continua. However, at microscopic scale these refractory materials involve sophisticated micro-structures that mix several phases. Generally, these micro-structures are composed by a large amount of inclusions embedded in a brittle matrix that ensures the cohesion of the material. In some cases, these materials can advantageously exhibit complex non linear mechanical behaviors that results from the interactions between the different phases that compose the composite micro-structure. These phenomena involve a high amount of discontinuities and can not be tackled easily with the Finite Element Method (FEM). The Discrete Element Method (DEM) naturally accounts for discontinuities and is therefore a good alternative to the continuum approaches such as the FEM. However, the difficulty with DEM is to perform quantitative simulations because the mechanical quantities can't be described in terms of the classical continuum theory such as stresses or strains. This study will describe the approach used to tackle this fundamental difficulty. The results given by the proposed approach are compared to experimental data obtained on simplified refractory materials.

Keywords: Refractories, Non linear mechanical behaviors, Discrete Element Method (DEM), Simulation, Calibration, Validation

I. INTRODUCTION

Rocks, ceramics or refractories are heterogeneous materials exhibiting a multi-phase composition involving different sizes of aggregates, bonding phases and additives. Most of these materials present numerous micro-cracks at room temperature resulting from thermal expansion mismatches between their various constituent phases and their thermal histories. These damages highly influence the thermo-mechanical properties of such materials. These phenomena can not be easily described with the Finite Element Method (FEM) which is not adapted to describe discontinuities at the microscopic scale [1], such as micro-cracks without assumptions on their localization, their paths, their growths and their coalescences.

The Discrete Element Method (DEM) could be an interesting alternative to study multi-damaged materials because it takes naturally into account discontinuities. The DEM implements a group of distinct elements (also named *discrete element*) that are in interaction through contacts or cohesive laws. This model consists of an assembly of discrete elements, deformable or not, linked up by simple mechanical laws to mimic the behavior of the material. The discrete element approach used here is a mix between the lattice models and the particle models as it was first proposed by Potyondy in [2]. The advantages are the description, in a natural way, of the crack initiations, the crack propagations, their coalescences and closures. However, the fundamental difficulty of this approach is to simulate quantitatively the continuum [2]. The purpose of the free DEM software GranOO is to face this difficulty. At this time, GranOO embeds some models that enable the quantitative simulation of mechanical, thermal and electrical behavior of continua with DEM [3][4][5].

The goal of this work is to find a fast and validated DEM calibration method to predict the occurrences of micro-cracks and their influences on macroscopic properties such as Young's modulus.

II. MODEL MATERIAL

The reference material used for this work is a *model material*. A model material mimics, through a simplified framework, a given decoupled phenomenon observed with real and complex materials. In order to study the impact of thermal expansion mismatches, a two-phase model material, composed of alumina inclusion and glass matrix, is preferred. The thermo-mechanical parameters values for alumina and glass were chosen to produce a micro-crack network during the cooling stage of the sample preparation.

The model materials used in this study are composed of spherical monomodal alumina inclusions (average diameter equals to 500 μm) which are randomly placed in a borosilicate glass matrix. The main requirements of the selected glass matrix are homogeneity, isotropy, a rather chemical inertia and the capability to adjust thermal expansion coefficient (CTE). In this way, a borosilicate glass has been prepared from the melting of a vitrifiable mixture initially constituted by different raw materials containing silica, boron oxide and other secondary oxides. A perfectly controlled volume fraction of alumina inclusions is incorporated in the mixture and is homogenized during 1 hour to ensure the dispersion of spherical alumina inclusions. Green specimens ($80 \times 40 \times 10 \text{ mm}^3$) are shaped by uni-axial pressing (80 MPa) before debinding and sintering under uni-axial pressure (15MPa at 600°C) to remove residual porosity. Three different volume fractions of inclusion were prepared (15%, 30% and 45%). Fig. 1 shows the microstructure of a final two-phase model material highlighting the micro-crack network. The main thermo-mechanical properties of both individual materials are given in the Tab.1.

Tab. 1. The main thermo-mechanical parameter values of the borosilicate glass and alumina

Properties	Matrix	Inclusion
Material	Glass	Alumina
Expansion coefficient α (K^{-1})	11.6×10^{-6}	7.6×10^{-6}
Young's modulus E (GPa)	72	340
Poisson's ratio ν	0.23	0.24
Tensile strength (MPa)	50	380

The introduction of spherical particles in the matrix leads the occurring of thermal stresses during the cooling stage of the sample processing. Because of the CTE mismatch, the matrix is under tensile mode and the inclusions are subjected to compressive stresses. Brittleness of the glass matrix induces orthoradial cracks that occurs and propagates in the matrix (Fig. 1).

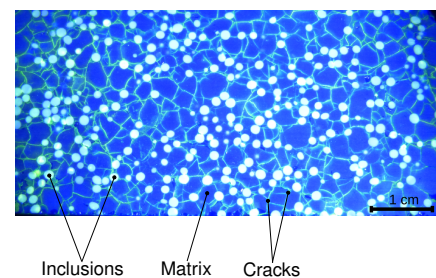


Fig. 1. Damaged microstructure of the model material

III. OVERVIEW OF THE NUMERICAL PROCEDURE

The main simulation steps implemented in this study is described in this section. The first step consists in calibrating the thermo-

mechanical parameters of the discrete element model (for details, see the next section). These microscopic parameters, related to the scale of the discrete elements, are denoted by the ‘ m ’ suffix. These parameters are the microscopic Young’s modulus E_m , radius ratio r_m (a geometrical factor which describes the link between the elements), tensile strength σ_{m_f} , thermal expansion coefficient (CTE) α_m and the coordination number cn (the average number of interaction (e.g., cohesive beams) per discrete element). In opposition, the emergent behaviors of the whole assembly network of discrete elements and the bounding shape of the discrete domain are called macroscopic. The macroscopic scale is symbolized by the ‘ M ’ suffix. These parameters are the macroscopic Young’s modulus E_M , Poisson’s ratio ν_M , tensile strength σ_{M_f} and CTE α_M . The macroscopic behavior corresponds to the behavior of the simulated materials. The values of microscopic parameters E_m , r_m , σ_{m_f} and α_m are quantified thanks to a calibration process in order to reach the required values of macroscopic parameters E_M , ν_M , σ_{M_f} and α_M . Considering the values reported in Tab.1, both borosilicate glass and alumina parameters are calibrated separately.

Concerning the relation between α_m and α_M , after carry out some simulations, the following simple result is obtained:

$$\alpha_\mu = \alpha_M \quad (1)$$

So, the thermal expansion coefficient can be introduced directly without any calibration. The calibration method of E_m , r_m is presented in the next section.

After building the initial cubic discrete domains, the second step consists in inserting the spherical alumina inclusions. This step involves a simple geometrical algorithm. Then, the virtual sample is cooled from 450°C (the glass transition temperature) to 20°C (room temperature). This step, that involves thermo-mechanical simulations, leads to cracks initiation and propagation in the virtual samples (see Fig. 2). In this study, the temperature is supposed constant within the sample and the thermal conduction is neglected. Finally, the damaged virtual samples given by the last step are “numerically frozen”, which means that further crack extension is forbidden. Thus, only the elastic behavior is taken into account. These “frozen samples” are submitted to virtual tensile tests to evaluate their apparent Young’s modulus E_M .

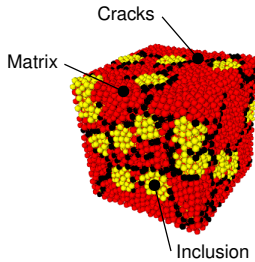


Fig. 2. Virtual sample of the two-phase model material

IV. FAST CALIBRATION METHOD OF ELASTIC PARAMETERS

The cohesive beam bond model [7] is used here to simulate elastic media characterized by Young’s modulus and Poisson’s ratio. In such model, the discrete elements are bonded by Euler-Bernoulli beams that can be loaded in a tensile, a bending and a torsion mode. The cohesive beams are simply defined by two microscopic parameters: a Young’s modulus E_m and radius ratio r_m . The radius ratio r_m is given by the ratio between the radius of cohesive beam and the average radius of the two discrete elements connected by this beam. The E_m and the r_m values are quantified thanks to a calibration process in order to reach the required values of macroscopic Young’s modulus E_M and Poisson’s ratio ν_M . The calibration process is a complicated and non-normalized process which uses trial-and-error method and requires a frustrating analysis related to several virtual tensile tests. This is the major obstacle on the use of DEM in industry and applied engineering numerical methods.

A fast and validated calibration method of E_m , r_m is presented in this section. The principle of this method is to find the relations between microscopic laws, at the discrete element scale and the macroscopic properties, at the structure scale, to skip the trial-and-error calibration.

Firstly, a series of numerical tensile tests with different values of microscopic parameters was performed in order to determine the relation between the macroscopic (E_M , ν_M) and microscopic parameters (E_m , r_m and cn) of the discrete element model.

Intervals of variation of E_m , r_m , cn are given in the Tab.2.

Tab. 2. Intervals of variation of microscopic parameters

Sample	Interval				Quantity											
	1	2	3	4												
E_m (GPa)	500	1000	1500	2000	2500	4										
r_m (-)	0.2	0.4	0.6	0.8	1.0	5										
cn (-)	5.5	6	6.5	7	7.5	8	8.5	9	9.5	10	10.5	11	11.5	12.5	13	16

Thus, $4 \times 5 \times 5 \times 16 = 1600$ tensile tests were performed to accomplish this task. Each tensile test gave one value of macroscopic Poisson’s ratio ν_M and one value of macroscopic Young’s modulus E_M . Consequently, a data cloud including 1600 data points was obtained. Based on this data cloud, analytical formulas were desired in order to best describe the relation between the DEM macroscopic and microscopic parameters.

A. Relation between macroscopic Poisson’s ratio ν_M and radius ratio r_m

According to the parametric study of Damien André in [6], there is an independence of the macroscopic Poisson’s ratio ν_M from microscopic Young’s modulus E_m . To study the evolution of the macroscopic Poisson’s ratio ν_M versus radius ratio r_m , for each value of coordination number, a scatter diagram is plotted (see Fig.3). In this diagram, the horizontal axis is related to values of r_m and the vertical axis is related to the corresponding values of ν_M . Based on this scatter, the non-linear least squares method is used to find out the best fitting function that well describes the considered evolution.

There are probably many functions which can describes this evolution. Consequently, the chosen fitting function must satisfy five criteria:

- 1) The maximum coefficient of determination must be obtained: $R^2 \in [0.98 : 1]$.
- 2) The maximum residual between the fitted curve and the scatter must be lower than 1%.
- 3) The fitting function must “work well” with all values of coordination number.
- 4) If many functions satisfy the three previous criteria, the function that involves the lowest number of coefficients is chosen.
- 5) The evolution of the related coefficients versus the coordination number must be describable by a fitting function. Chaotic evolutions are proscribed.

After trial-and-error proceeding, one found that the relation $\nu_M = f_1(r_m)$ could be well described by a third order approximate function (see equation 2 and Fig.3):

$$\nu_M = f_1(r_m) = a_1 + b_1 \cdot r_m + c_1 \cdot r_m^2 + d_1 \cdot r_m^3 \quad (2)$$

The five proposed criteria are perfectly satisfied by equation 2.

B. Relation between macroscopic Young’s modulus E_M and radius ratio r_m and microscopic Young’s modulus E_m

The same approach used in the previous section is used here. For each value of coordination number, a 3D scatter diagram is plotted (see Fig.4). In this diagram, the two horizontal axis are related to values of r_m and E_m , and the vertical axis is related to the corresponding values of E_M . Based on this 3D scatter, the non-linear least squares method is used again to find out the best fitting function that well describes the evolution of macroscopic

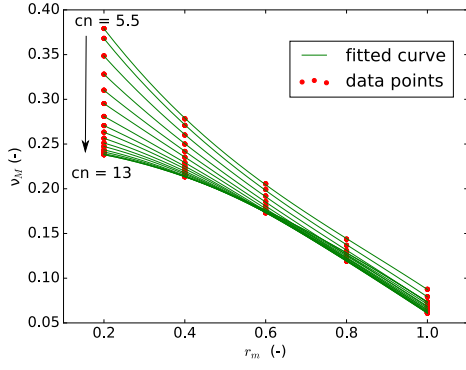


Fig. 3. Fitted curve corresponding to all values of coordination number

Young's modulus E_M versus radius ratio r_m and microscopic Young's modulus E_m . The chosen function must satisfy the five criteria as explained in the section IV-A.

After trial-and-error proceeding, one found that the relation $E_M = f_2(E_m, r_m)$ could be well described by the following analytic formula:

$$E_M = f_2(E_m, r_m) = E_m \cdot (a_2 + b_2 \cdot r_m + c_2 \cdot r_m^2 + d_2 \cdot r_m^3) \quad (3)$$

The five proposed criteria are perfectly satisfied by equation 3 (see Fig.4).

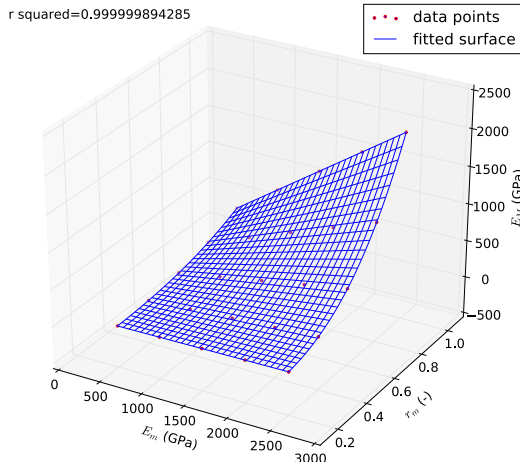


Fig. 4. Case of coordination number $cn = 6$

C. Relation between the macroscopic parameters and coordination number

In the two previous sections, the functions f_1 , f_2 which express the relation between the macroscopic parameters (E_M, ν_M) and the microscopic parameters (E_m, r_m) of discrete element model were successfully found (see equations 2 and 3). However, their coefficients a_1, b_1, c_1, d_1 and a_2, b_2, c_2, d_2 depend on the coordination number. The aim of this section is to find the relations between these coefficients and the coordination number.

The non-linear least squares method is used once again to find out the best fitting functions that well describe the considered relations. Scatters of data are plotted (Fig.5 and Fig.6). In each scatter, the horizontal axis is related to values of coordination number, the vertical axis is related to the corresponding values of the considered coefficient. The first fitting function $\nu_M = f_1(r_m)$ involves 4 coefficients a_1, b_1, c_1, d_1 . Therefore, 4 fitting functions which express the evolutions of these 4 coefficients need to be found. The similar process is performed for the second fitting function $E_M = f_2(E_m, r_m)$. There are also 4 fitting functions for 4 coefficients a_2, b_2, c_2, d_2 .

There are probably many functions which can describes these evolutions. Consequently, the chosen fitting function related to each coefficient must satisfy three criteria:

- 1) The maximum coefficient of determination must be obtained: $R^2 \in [0.98 : 1]$
- 2) If many functions satisfy the previous criterion, the function that involves the lowest number of coefficients is chosen.
- 3) The fitting function "work well" with all coefficients related.

After trial-and-error proceeding, expressions of the relation between the considered coefficients and coordination number are found (see formulas 4, 5):

$$coe_{f_1} = g_1(cn) = A_1 + B_1 \cdot \tanh[C_1 \cdot (cn - 7) + D_1] \quad (4)$$

$$coe_{f_2} = g_2(cn) = A_2 + B_2 \cdot cn + C_2 \cdot cn^2 + D_2 \cdot cn^3 \quad (5)$$

In the formula 4 and 5: coe_{f_1}, coe_{f_2} represents (a_1, b_1, c_1, d_1) and (a_2, b_2, c_2, d_2) respectively. The three proposed criteria are perfectly satisfied by these formulas. The fitted curves and their representative equations are shown in Fig.5 and 6.

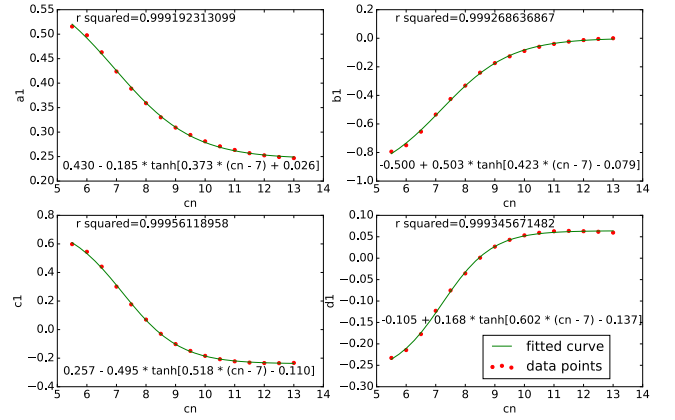


Fig. 5. Fitted curves for coefficients of $\nu_M = f_1(r_m)$

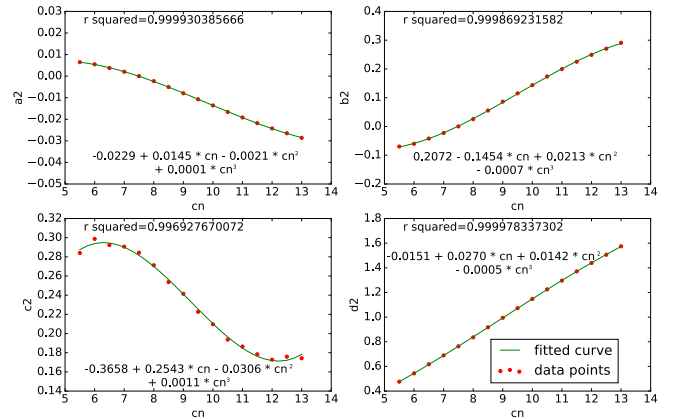


Fig. 6. Fitted curves for coefficients of $E_M = f_2(E_m, r_m)$

D. Validation of the proposed relation between macroscopic parameters and coordination number

To validate the proposed relation between macroscopic parameters and coordination number, a series of virtual tensile tests were performed. In this study, the validation process were accomplished for glass and alumina.

For each value of coordination number, coefficients of two fitting functions $\nu_M = f_1(r_m)$ and $E_M = f_2(E_m, r_m)$ (i.e., a_1, b_1, c_1, d_1 and a_2, b_2, c_2, d_2 respectively) were calculated by using functions $g_1(cn)$ and $g_2(cn)$ respectively (see equations 4 and 5).

Thanks to these values of coefficients and values of macroscopic parameters of simulated materials (i.e., glass and alumina, see Tab.1), values of E_m, r_m are computed (equation 6).

$$\begin{cases} a_1 + b_1 \cdot r_m + c_1 \cdot r_m^2 + d_1 \cdot r_m^3 = \nu_M \\ E_m \cdot (a_2 + b_2 \cdot r_m + c_2 \cdot r_m^2 + d_2 \cdot r_m^3) = E_M \end{cases} \quad (6)$$

In equation 6, a_1, b_1, c_1, d_1 and a_2, b_2, c_2, d_2 are computed by using functions $g_1(cn)$ and $g_2(cn)$ respectively. Value of ν_M and E_M are given by Tab.1.

Thus, for each value of coordination number, values of microscopic parameters (E_m, r_m) are obtained for the two simulated materials. These values were used to perform virtual tensile tests. The macroscopic Young's modulus and Poisson's ratio obtained by these tests were compared to the required values of the corresponding parameters of glass and alumina (Tab.1). If the maximum residual between the values obtained by validation tests and the required values is lower than 2%, the proposed relation will be validated.

Synthesis of the validation process is shown in the Tab.3 and 4.

Tab. 3. Validation results for glass

cn	r_m computed (-)	E_m computed (GPa)	ν_M obtained (-)	Residual (%)	E_M obtained (GPa)	Residual (%)
5.5	0.524	617.76	0.231	0.633	71.90	0.134
6	0.506	593.49	0.231	0.533	72.26	0.366
6.5	0.485	586.61	0.230	0.001	71.76	0.320
7	0.461	591.98	0.230	0.103	72.00	0.001
7.5	0.438	603.58	0.230	0.145	71.97	0.035
8	0.417	615.98	0.230	0.125	71.56	0.608
8.5	0.398	626.40	0.230	0.082	71.83	0.226
9	0.380	635.17	0.230	0.030	72.43	0.594
9.5	0.364	644.15	0.230	0.257	71.93	0.091
10	0.348	654.66	0.230	0.167	71.74	0.363
10.5	0.333	666.57	0.230	0.151	71.63	0.516
11	0.320	678.49	0.230	0.191	71.33	0.926
11.5	0.308	688.53	0.230	0.072	71.15	1.181
12	0.298	695.11	0.230	0.112	70.86	1.573
12.5	0.290	697.40	0.230	0.184	70.98	1.421
13	0.283	695.47	0.230	0.163	70.87	1.572

Tab. 4. Validation results for alumina

cn	r_m computed (-)	E_m computed (GPa)	ν_M obtained (-)	Residual (%)	E_M obtained (GPa)	Residual (%)
5.5	0.497	3381.77	0.241	0.442	339.78	0.066
6	0.478	3268.05	0.241	0.474	341.36	0.399
6.5	0.456	3255.69	0.240	0.067	338.88	0.328
7	0.432	3320.71	0.240	0.148	339.90	0.028
7.5	0.407	3435.92	0.240	0.245	339.74	0.077
8	0.383	3578.274	0.240	0.041	337.62	0.700
8.5	0.360	3739.90	0.240	0.167	338.88	0.328
9	0.338	3931.21	0.240	0.016	341.69	0.491
9.5	0.316	4173.29	0.241	0.329	338.88	0.328
10	0.294	4487.15	0.241	0.304	337.57	0.714
10.5	0.272	4887.17	0.241	0.299	336.82	0.934
11	0.251	5378.78	0.241	0.335	335.47	1.332
11.5	0.232	5957.74	0.240	0.007	335.42	1.346
12	0.214	6609.49	0.240	0.116	336.18	1.122
12.5	0.199	7308.56	0.239	0.283	340.39	0.115
13	0.187	8020.02	0.239	0.361	345.09	1.500

As we can see in the Tab.3 and 4, residuals are very low. The maximum residual is 1.57%. Consequently, the proposed relations between macroscopic parameters and microscopic parameters of discrete element model are validated.

V. RESULTS AND CONCLUSION

Following the approach described in the section III, discrete domains were subjected to cooling tests and then, to tensile tests in order to quantify their apparent Young's modulus. During the tensile tests, the micro-cracks are "frozen" and are not allowed to extend. Experimentally, the Young's modulus are measured by ultrasonic pulse echography technique that do not damage the materials. Finally, the results of numerical simulations and experimental observations are plotted in Fig. 7, where: the absciss *Volume fraction* is the volumic fraction of inclusion in samples, the Hv^- and Hv^+ curves denote bounds of the Hashin & Shtrikman (H&S) model [8], the *Numerical 3D model without cracks* curve corresponds to the undamaged DEM samples, the *Numerical 3D model with cracks* curve corresponds to the damaged DEM samples and the *Experimental* curve corresponds to the experimental observations.

These results shows that the *Numerical 3D model without cracks* match perfectly with the H&S model which does not take into

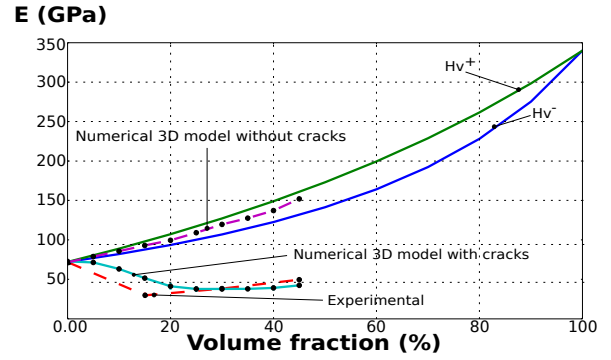


Fig. 7. Comparison of Young's modulus between experimental, numerical results and H&S model

account damages inside material. However, the *Numerical 3D model with cracks* match with the experimental results measured by ultrasonic pulse echography technique. It allows to validate quantitatively the numerical 3D DEM model.

This work related to the simulation of thermo-elastic behavior using DEM presents a significant improvement of the discrete element methods applied to the simulation of continuum media. This model has been applied to study the influence of damage generated during the cooling stage of multiphase materials. This damage highly influences the rigidity of materials and is a high level of importance for common engineering applications. The proposed method seems to be adapted to predict this rigidity and allows to consider further studies to improve the understanding of more complex multiphase materials such as refractories.

Accuracy of the DEM simulation depends entirely on how accurately the microscopic parameters are selected. A fast calibration method is proposed and validated in the section IV. For the further work, the accuracy of the proposed method need to be carefully checked by changing several factors such as: shape and/ or size of discrete domain, number of discrete elements, etc. Furthermore, a similar work on the tensile strength need to be accomplish in the future study.

ACKNOWLEDGEMENTS

This study was conducted within the framework of FIRE (Federation of International Refractory Research and Education), project Delta. Financial support from the Nouvelle-Aquitaine region (France) is gratefully acknowledged.

REFERENCES

- [1] Babuška I, Andersson B, Guo B, Melenk JM, Oh HS. Finite element method for solving problems with singular solutions. *Journal of computational and applied mathematics*. 1996 Nov 5;74(1-2):51-70.
- [2] Potyondy DO, Cundall PA. A bonded-particle model for rock. *International journal of rock mechanics and mining sciences*. 2004 Dec 31;41(8):1329-64.
- [3] André Damien, Jean-Luc Charles, and Ivan Iordanoff. 3D Discrete Element Workbench for Highly Dynamic Thermo-mechanical Analysis: Gran00. Vol. 3. John Wiley & Sons, 2015.
- [4] Hubert C, André D, Dubar L, Iordanoff I, Charles JL. Simulation of continuum electrical conduction and Joule heating using DEM domains. *International Journal for Numerical Methods in Engineering*. 2016 Jan 1.
- [5] Terreros I, Iordanoff I, Charles JL. Simulation of continuum heat conduction using DEM domains. *Computational Materials Science*. 2013 Mar 31;69:46-52.
- [6] André Damien. Modélisation par éléments discrets des phases d'ébauche et de doucissage de la silice. Université de Bordeaux PhD Thesis. 2012.
- [7] André D, Iordanoff I, Charles JL, Néauport J. Discrete element method to simulate continuous material by using the cohesive beam model. *Computer Methods in Applied Mechanics and Engineering*. 2012 Mar 1;213:113-25.
- [8] Hashin Z, Shtrikman S. A variational approach to the theory of the elastic behaviour of multiphase materials. *Journal of the Mechanics and Physics of Solids*. 1963 Mar 1;11(2):127-40.